Earth Planets Space, **58**, 601–605, 2006

A comparative study of the bottomside profile parameters over Wuhan with IRI-2001 for 1999–2004

Huajiao Chen[1,2,3], Libo Liu[1], Weixing Wan[1], Baiqi Ning[1], and Jiuhou Lei[1]

[1]*Division of Geomagnetism and Space Physics, Institute of Geology and Geophysics, Chinese Academy of Sciences, Beijing 100029, China*
[2]*Wuhan Institute of Physics and Mathematics, Chinese Academy of Sciences, Wuhan, China*
[3]*Graduate School of Chinese Academy of Sciences, Beijing 100049, China*

(Received August 30, 2005; Revised October 21, 2005; Accepted October 25, 2005; Online published May 12, 2006)

The diurnal, seasonal, and solar activity variations of the bottomside ionospheric profile parameters $B0$ and $B1$ are studied using electron density profiles measured over Wuhan (30.4°N, 114.4°E) of China with a DGS-256 Digisonde during 1999–2004. Comparisons are made with the International Reference Ionosphere model (IRI-2001) using both the standard option ($B0$-Tab and $B1$-Tab) and the Gulyaeva's option ($B0$-Gul and $B1$-Gul). The results show that: (1) observed $B0$ has distinct diurnal and seasonal variations, while observed $B1$ changes little with season. The value of $B0$ is larger in summer than that in equinox and winter, especially for daytime. In winter and equinox, $B0$ also presents morning and afternoon collapses as reported by Lei *et al.* (2004). (2) $B0$ increases about 18.6 km from low solar activity (LSA) to high solar activity (HSA). $B1$ in HSA is smaller than that in LSA before 10:00 LT and with an opposite tendency during the rest time. (3) Observed $B0$ is in better agreement with $B0$-Gul than with $B0$-Tab, though the $B0$-Gul overestimates during 09:00 to 17:00 LT in equinox and summer. $B0$-Tab is 12–20 km larger than the observations over Wuhan almost all the time. Meanwhile, $B1$-Tab is in good agreement with the observations.

Key words: Low latitude ionosphere, DGS-256 Digisonde, IRI model, modeling and forecasting.

1. Introduction

The International Reference Ionosphere (IRI) model is a global empirical model which specifies the monthly average of the electron density, electron and ion temperatures, and ion compositions (Bilitza, 2001). Over the past decades, the Committee on the Space Research (COSPAR) and the International Union of Radio Science (URSI) who established the IRI models have released a series of IRI models. The most updated IRI-2001 (Bilitza, 2001) has been made great improvements. As to the bottomside region, these improvements include a better description of the occurrence statistics of F_1 layer (Scotto *et al.*, 1997, 1998), a new table of values of $B0$ and $B1$ (Bilitza *et al.*, 2000), and a better description of the transition region from the bottomside to the E valley (Reinisch and Huang, 1999).

The electron density profile $N_e(h)$ of the bottomside ionosphere in the IRI model was described by the following expression (Ramakrishnan and Rawer, 1985),

$$N_e = N_m F_2 \exp(-x^{B1})/\cosh(x),\ x = (h_m F_2 - h)/B0, \quad (1)$$

Here $B0$ is the thickness parameter and $B1$ a shape parameter of the bottomside ionospheric profile.

The profiles are fitted with Eq. (1) from $h_m F_2$ to $h_{0.24}$ (the height where the density falls to 0.24 times of $N_m F_2$) to obtain the $B0$ and $B1$ if no F_1-layer exists, or to the F_1 peak if F_1-layer occurs. The IRI model offers two options to provide $B0$ and $B1$. The standard option of $B0$ ($B0$-Tab) uses a table of $B0$ values deduced from profile inversion of ionograms at mid-latitude stations, and the Gulyaeva's option ($B0$-Gul) based on the half density height $h_{0.5}$ (Gulyaeva, 1982). While the standard option of $B1$-Tab is analytical, and the Gulyaeva's option ($B1$-Gul) is a constant 3.

In the Gulyaeva's opinion, $B0$ can be given as

$$B0 = (h_m F_2 - h_{0.5})/C. \quad (2)$$

Here C is a function of $B1$. Since $B1$-Gul is a constant value of 3, so C is a constant value too. Therefore, $B0$-Gul is proportional to the value of $h_m F_2$ minus $h_{0.5}$.

The objective of this paper is to analyze the diurnal, seasonal, and solar activity variations of $B0$ and $B1$ using the Digisonde observations over Wuhan during the period 1999–2004. Then a comparison between the observations and the IRI-2001 model is made to validate the new updated IRI model over Wuhan.

2. Data and Analysis Method

Since 1946, ionosonde measurements have been routinely made at Wuhan (geographic 114.4°E, 30.6°N; 45.2° dip) which located in central China, is just away from the northern crest of equatorial anomaly in East Asia. It has significant values for studying low latitude ionospheric dynamics (e.g., Liu *et al.*, 2003, 2004). A DGS-256 Digisonde started routinely measuring the ionosphere over Wuhan after its update in 1999. The present paper uses a database of more than 200,000 ionograms collected during 1999 to 2004. Huge effort has been made to manually scale

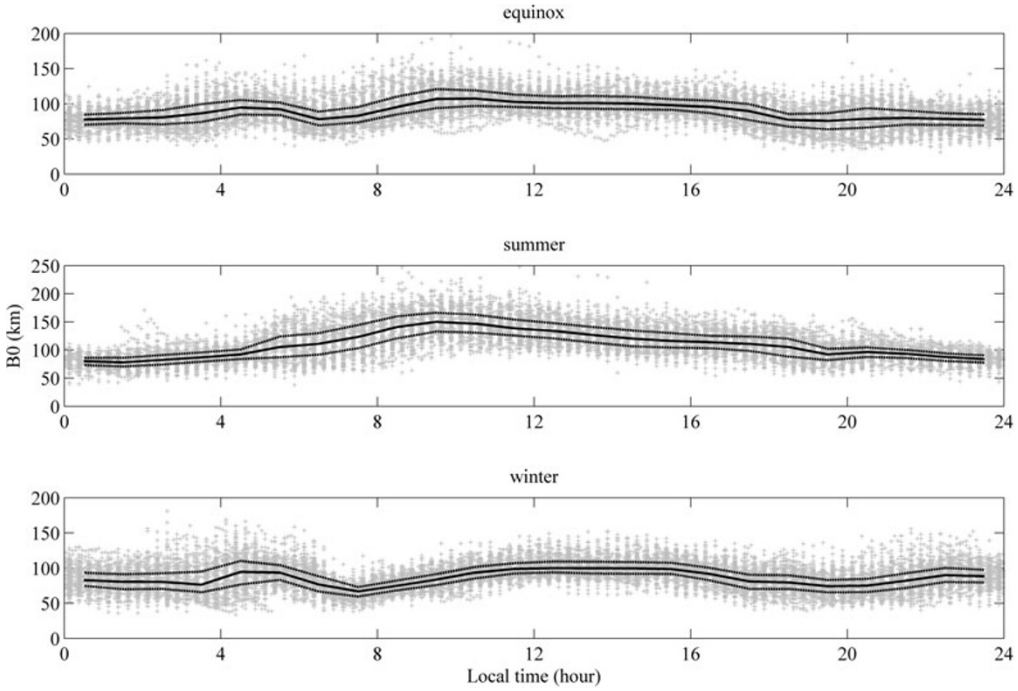

Fig. 1. Diurnal and seasonal variations of the thickness parameter $B0$ derived from Wuhan DGS-256 observations under the high solar activity. The median results are shown as solid lines; along with the upper quartile UQ and lower quartile LQ (dashed lines) of $B0$ values.

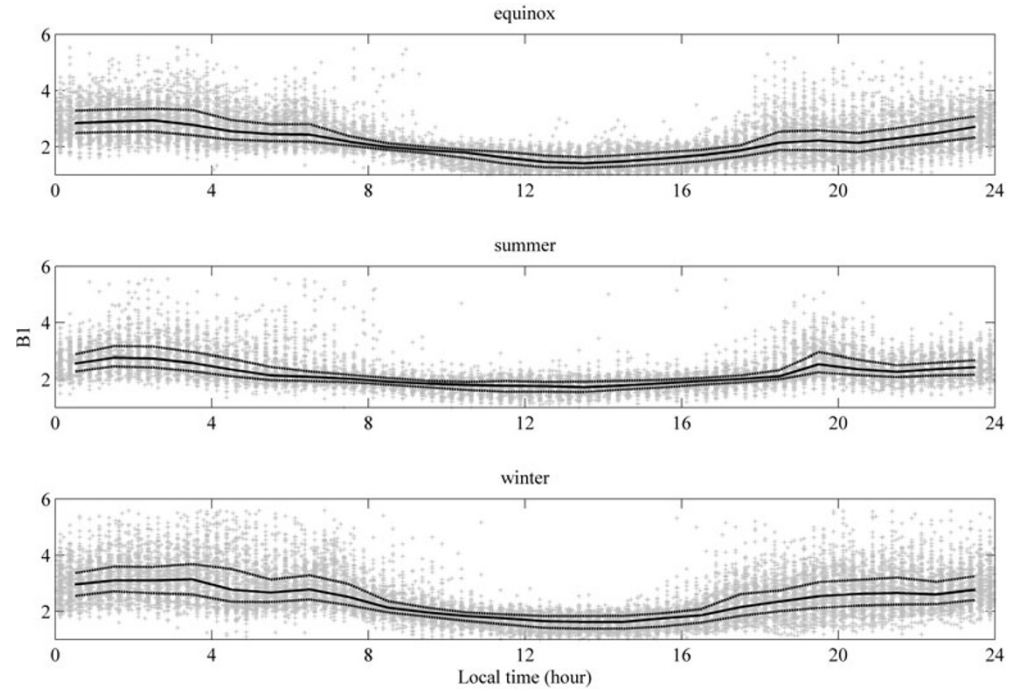

Fig. 2. Diurnal and seasonal variations of the shape parameter $B1$ derived from Wuhan DGS-256 observations under the high solar activity. The median results are shown as solid lines; along with the upper quartile UQ and lower quartile LQ (dashed lines) of $B1$ values.

those ionograms, and then bottomside profiles are calculated from these manual-scaling ionograms with a standard "true height" inversion program (Huang and Reinisch, 1996) inherent in the UMLCAR SAO-Explorer. At the same time, critical frequency of the F layer (foF_2), its height (h_mF_2), and other parameters (i.e., the profile parameters $B0$ and $B1$, etc.) are then obtained.

We use the data basically on magnetically quiet to moderate conditions with the 3-hourly planetary geomagnetic index $ap < 20$. They are grouped according to their season and solar activity, that is, May-August for summer, November-February for winter and others for equinox; $F_{10.7p} = (F_{10.7} + F_{10.7A})/2 > 170$ for high solar activity (HSA), and $F_{10.7p} = (F_{10.7} + F_{10.7A})/2 < 130$ for low solar activity (LSA).

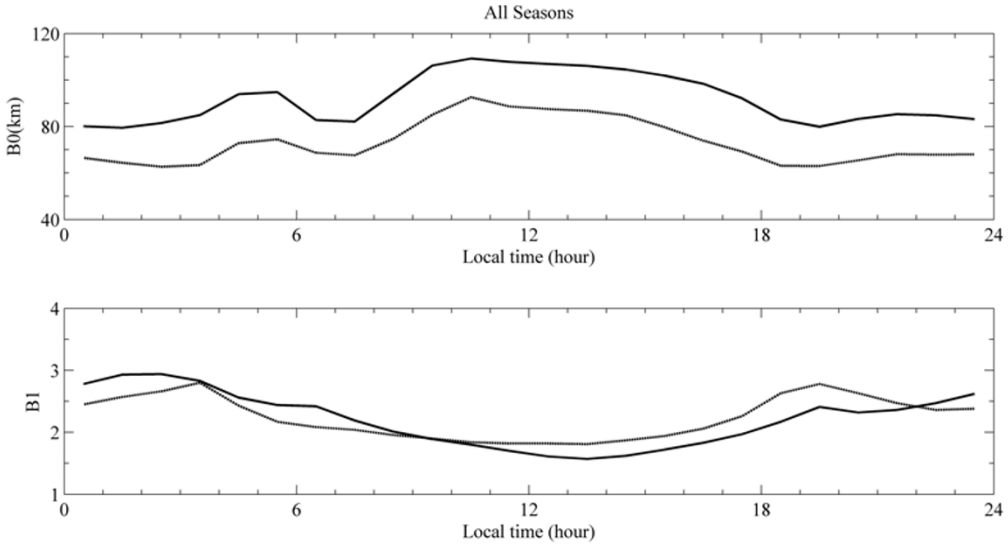

Fig. 3. Diurnal variation of the $B0$ and $B1$ derived from Wuhan DGS-256 observations under low and high solar activity. The high solar activity median results are shown as solid lines; the low solar activity median results are shown as dash line.

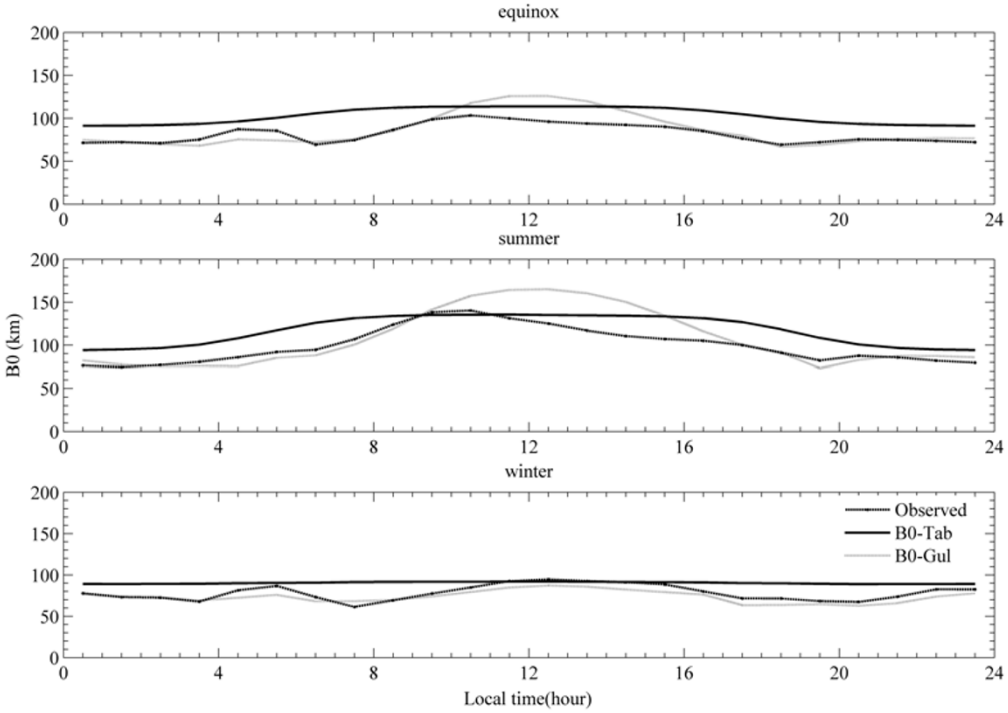

Fig. 4. Comparisons of the median values of $B0$ obtained from the Wuhan DGS-256 measurements with $B0$-Tab (solid lines), and $B0$-Gulyaeva (dashed lines) predicted by the IRI model.

3. Results

3.1 Observed *B* parameters

Figure 1 displays the diurnal and seasonal variations of the thickness parameter $B0$ under HAS against local time, the corresponding median values, upper (UQ) and lower (LQ) quartiles are also given. From the scatter plots, it can be seen that in summer daytime $B0$ shows a large scatter. During summer, the median value of $B0$ varies from around 80 km at 00:00 LT to diurnal peak of 150 km around 09:00 LT, and thereafter, it falls gradually to 80 km around midnight. In winter, the median $B0$ increases from 76 km (around 03:30 LT) to 92 km (around 04:30 LT), then falls to 68 km (around 07:30 LT), after that it increases again to 100 km (around 12:40 LT), and falls gradually until 20:00 LT. In equinox, the values of median $B0$ are similar as those in winter. They both have an increasing trend before 05:00 LT and have morning and afternoon collapses which are stronger in winter than in equinox and weaker in afternoon than in morning. These diurnal variations of $B0$ in winter and equinox were found over Millstone Hill (Lei *et al.*, 2004). The diurnal and seasonal variation of the shape parameter $B1$ under HSA against local time are shown in Fig. 2, along with median values, upper quartile (UQ) and lower quartile (LQ). Comparing with $B0$, $B1$ depicts more

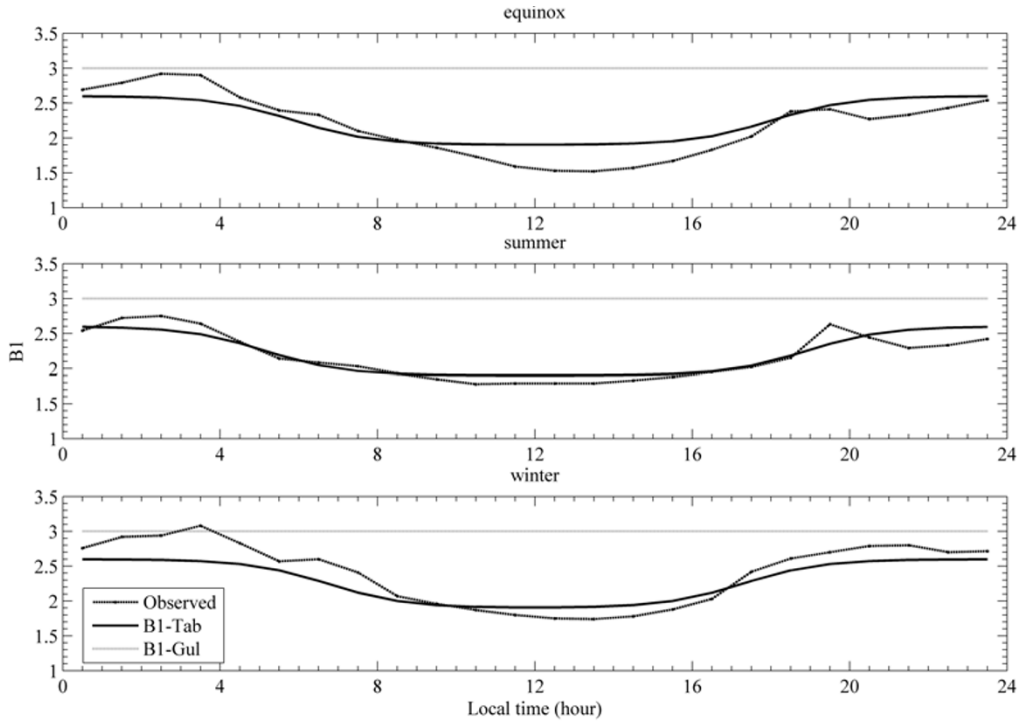

Fig. 5. Comparisons of the median values of $B1$ obtained from the Wuhan DGS-256 measurements with $B0$-Tab (solid lines), and $B0$-Gulyaeva (dashed lines) predicted by the IRI model.

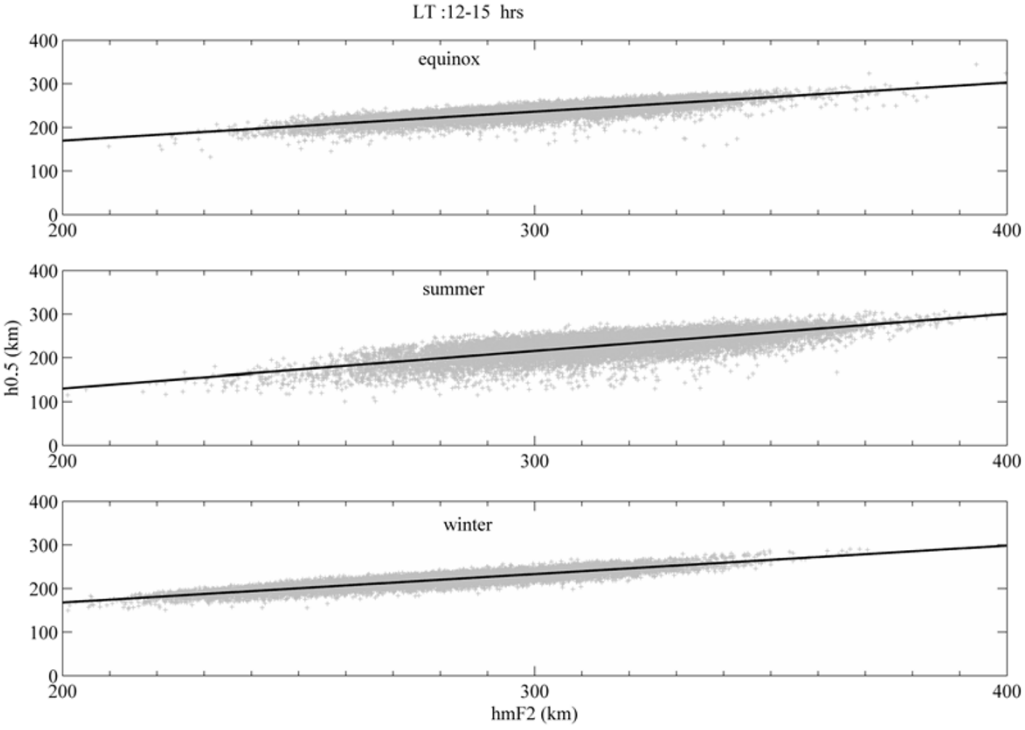

Fig. 6. Scatter plots of h_mF_2 against $h_{0.5}$ and their best fits are given during 12:00 to 15:00 LT for equinox, summer and winter.

scattered, especially during the night. $B1$ is higher in winter at night and lower in summer during the daytime. Generally, $B1$ varies between 1 and 6, and the median value of $B1$ is about 1.89 in the day and 2.54 at the night.

Diurnal variations of the median $B0$ and $B1$ for all the seasons under high (solid lines) and low (dash lines) solar activity levels are plotted in Fig. 3. The upper panel shows the plots of $B0$, the lower panel shows the plots of $B1$. From the upper panel, it can be seen that from HSA to LSA, the mean increase of $B0$ is 18.6, the minimum is 13.6, and the maximum is 24.5. This solar activity dependence is consistent with the results of Lei *et al*. (2004) and Sethi and Mahajan (2002). From the lower panel, the results display that in the HSA $B1$ is smaller during 00:00 to 10:00 LT,

and its tendency is opposite during the rest time. This solar activity dependence of $B1$ is not consistent with Sethi and Mahajan (2002) and Lei *et al.* (2004). In Arecibo (Sethi and Mahajan 2002), the LSA $B1$ is larger, but in Millstone Hill (Lei *et al.*, 2004) the HSA $B1$ is larger. Since the mean $F_{10.7p}$ under high solar activity is 194, and the mean $F_{10.7p}$ under low solar activity is 122 which is much larger than common mean $F_{10.7p}$ of low solar activity, so further investigations are needed.

3.2 Comparison with IRI model

Figure 4 shows comparisons of the median values of $B0$ obtained from Wuhan DGS-256 measurements with that of $B0$-Tab (solid lines), and $B0$-Gulyaeva (dash lines) predicted by the IRI-2001. It can be seen that $B0$-Gul agrees with the observations well, especially in winter, while $B0$-Tab mostly overestimates the observations. In equinox and summer $B0$-Gul overestimates the observations in the daytime. In the earlier studies, Mahajan *et al.* (1995) also reported that during solar minimum period (1974–1977) $B0$-Gul were significantly larger during daytime in equinox and summer. $B0$-Tab represents the diurnal variation not quite well, particularly in winter when the median values of $B0$-Tab are unchanged. $B0$-Tab results are somewhat different from those in Wuhan (Zhang and Huang, 1998) and Hainan (Zhang *et al.*, 2004), in which both observation-based $B0$ is systematically larger by day and smaller by night than IRI's. $B0$-Tab mean overestimates by 12–20 km, but that of $B0$-Gul is about 5–12 km.

Comparisons of the median values of $B1$ with $B0$-Tab (solid lines), and $B0$-Gul (dash lines) predicted by the IRI-2001 are showed in Fig. 5. $B1$-Gul has constant value of 3. $B1$-Tab agrees with observations well particularly in summer. In equinox before 08:00 LT, it underestimated the observations, after that it overestimated the observations. In winter, it underestimated at the night, and overestimate in the day. These results are quite similar with those in Hainan, China (Zhang *et al.*, 2004).

As above $B0$-Gul is always significantly larger during daytime in equinox and summer, and $B0$-Gul was based on the half density point $h_{0.5}$, so we have examined the relationship between h_mF_2 and $h_{0.5}$ for equinox, summer and winter. Figure 6 shows scatter plots of h_mF_2 against $h_{0.5}$ and their best fits during 12:00 to 15:00 LT for equinox summer and winter. It can be seen that in summer the scatter is larger. It can explain the $B0$-Gul deviations in summer. Mahajan *et al.* (1995) has also found that during daytime the lower values of $h_{0.5}$ are often coincident, whenever there is F_1 layer between $h_{0.5}$ and h_mF_2.

4. Summary and Conclusion

Electron density profiles measured with DGS-256 Digisonde over Wuhan station are used to obtain the F_2 bottomside parameters $B0$ and $B1$ during the period from 1999 to 2004. Median values of these two parameters are made to compare with the newly updated IRI-2001. The results show that: (1) $B0$ has distinct diurnal and seasonal variations, while $B1$ changes little with seasons. The value of $B0$ is larger in summer than that in equinox and winter, especially for daytime. In winter and equinox, $B0$ also presentes morning and afternoon collapses as reported by Lei *et al.* (2004). (2) $B0$ increases about 18.6 km from LSA to HSA. $B1$ in HSA is smaller than that in LSA before 10:00 LT, and its tendency is opposite during the rest time. This solar activity dependence of $B1$ is somewhat different from previous studies (Lei *et al.*, 2004; Sethi and Mahajan, 2002). (3) Our $B0$ observations are in better agreement with the $B0$-Gul option than with the $B0$-Tab, though the $B0$-Gul option overestimates the observed $B0$ during 09:00 to 17:00 LT in equinox and summer. $B0$-Tab is larger than the observations 12–20 km over Wuhan almost all the time. Meanwhile, $B1$-Tab is in good agreement with the observations.

Acknowledgments. This research was supported by the KIP Pilot Project (kzcx3-sw-144) of Chinese Academy of Sciences and National Natural Science Foundation of China (40574071, 40574072).

References

Bilitza, D., International Reference Ionosphere 2000, *Radio Sci.*, **36**(2), 261–275, 2001.

Bilitza, D., S. Radicella, B. Reinish, J. Adeniyi, M. Mosert de Gonzalez, S. Zhang, and O. Obrou , New B0 and B1 models for IRI, *Adv. Space Res.*, **25**(1), 86–96, 2000.

Gulyaeva, T. L., Implementation of a new characteristic parameter into the IRI sub-peak electron density profile, *Adv. Space Res.*, **2**(10), 191–194, 1982.

Huang, X. and B. W. Reinisch, Vertical electron density profiles from the digisonde network, *Adv. Space Res.*, **18**(6), 121–129, 1996.

Lei, J., L. Liu, W. Wan, S.-R. Zhang, and J. M. Holt, A statistical study of ionospheric profile parameters derived from Millstone Hill incoherent scatter radar measurements, *Geophys. Res. Lett.*, **31**, L14804, doi:10.1029/2004GL020578, 2004.

Liu, L., W. Wan, X. Luan, B. Ning, and J. Lei, Solar activity dependence of the effective winds derived from ionospheric data at Wuhan, *Adv. Space. Res.*, **32**, 1719–1724, 2003.

Liu, L., W. Wan, C. C. Lee, B. Ning, and J. Y. Liu, The low latitude ionospheric effects of the April 2000 magnetic storm near the longitude 120°E, *Earth Planets Space*, **56**, 607–612, 2004.

Mahajan, K. K., R. Kohli, N. K. Sethi, and V. K. Pandey, Variability of the F-region parameter $h_{0.5}$, *Adv. Space Res.*, **15**(1), 51–60, 1995.

Ramakrishnan, Y. V. and K. Rawer, Electron density reference profile in the lower ionosphere, *Adv. Space Res.*, **5**(7), 29–34, 1985.

Reinish, B. and X. Huang, Redefining the IRI F1 layer profile, *Adv Space Res.*, **25**(1), 81–88, 1999.

Scotto, C., M. Mosert de Gonzalez, S. Radicella, and B. Zolesi, On the prediction of the F1 ledge occurrence and critical frequency, *Adv. Space Res.*, **20**(9), 1773–1776, 1997.

Scotto, C., Radicella, and B. Zolesi, An improved probability function to predict the F1 layer occurrence and critical frequency, *Radio sci.*, **33**, 1763–1765, 1998.

Sethi, N. K. and K. K. Mahajan, The bottomside parameters B0, B1 obtained from incoherent scatter measurements during a solar maximum and their comparisons with the IRI-2001 model, *Ann. Geophys.*, **20**(6), 817–822, 2002.

Sethi, N. K. and V. K. Pandey, Comparative study of electron density from incoherent scatter measurements at Arecibo with the IRI-95 model during solar maximum, *Ann. Geophys.*, **20**, 817–822, 2004.

Zhang, M. L., J. K. Shi, X. Wang, S. Z. Wu, and S. R. Zhang, Comparative study of ionospheric characteristic parameters obtained by DPS-4 digisonde with IRI-2000 for low latitude station in china, *Adv. Space Res.*, **33**, 869–873, 2004.

Zhang, S.-R. and X.-Y. Huang, Variations of bottomside electron density profile parameters obtained from observations at Wuchang, China, *Adv. Space Res.*, **22**(6), 749–752, 1998.

H. Chen, L. Liu (e-mail: liul@mail.iggcas.ac.cn), W. Wan, B. Ning, and J. Lei